ELSEVIER

Polymer 42 (2001) 6587–6597

polymer

www.elsevier.nl/locate/polymer

On the crystallization, morphology and physical properties of a clarified propylene/ethylene copolymer

Y. Zhao[a], A.S. Vaughan[b,*], S.J. Sutton[c], S.G. Swingler[c]

[a]*J.J. Thomson Physical Laboratory, The University of Reading, Reading RG6 6AF, UK*
[b]*Department of Electronics and Computer Science, University of Southampton, Highfield, Southampton SO17 1BJ, UK*
[c]*National Grid, Engineering and Technology, Kelvin Avenue, Leatherhead KT22 7ST, UK*

Received 31 May 2000; received in revised form 27 November 2000; accepted 4 January 2001

Abstract

The crystallization behaviour, morphology and electrical and mechanical properties of a propylene/ethylene copolymer containing a clarifying additive have been studied. The addition of the clarifier generally results in enhanced nucleation and consequent formation of a more uniform structure. The melting behaviour is analysed and it is shown that, only following quenching, are the observed multiple melting peaks associated with dynamic reorganization effects. Otherwise, the various endotherms are associated with the initial crystallization process itself. The morphology of the copolymer is shown to change abruptly from a fine to a coarse structure when the crystallization temperature exceeds 128°C. This is associated with a marked reduction in the nucleating efficiency of the additive, which permits the growth of distinct, spatially separated morphological features that are best termed quadrites. Through a combination of the increased crystallization temperature and the growth of these relatively large structural units, appreciable molecular fractionation is also observed. These changes in crystallization behaviour should have important consequences for the macroscopic physical properties; dielectric breakdown and mechanical failure have been investigated. Although the electric strength of the material exhibits a clear dependence on sample morphology, most of the mechanical parameters do not vary in the same discontinuous manner. The only significant correlations seen between electrical and mechanical parameters involve the ultimate failure stress and strain, as recorded at a relatively high strain rate of 100 mm/min. Consequently, although this suggests that dielectric breakdown and mechanical failure may be weakly related, no agreement with existing theoretical predictions has been found.

Keywords: Propylene/ethylene copolymer; Nucleation; Morphology

1. Introduction

Dielectric breakdown phenomena pose major scientific and technological problems in areas ranging from semiconductor manufacture to high voltage power engineering. Although much work has been conducted in this area, fundamental understanding is, nevertheless, poor. Indeed, many results are even contradictory, most probably as a direct consequence of the use of poorly controlled materials. For example, although many attempts have been made to investigate the role of morphology [1–6], these have generally involved ill-defined systems, in which a range of factors could have affected the results. Nevertheless, recent experimental work involving a high degree of material design has clearly indicated how reproducible results can be obtained and has, simultaneously, begun to demonstrate the way in which structural factors influence the electric strength of semi-crystalline polymers [7]. However, whilst short-term electrical properties are of academic interest, over longer time scales and at lower applied fields, it is the formation of fractal structures termed electrical trees that leads to the eventual failure of polymeric insulation. The investigation of tree growth in polymers is, consequently, of both academic and technological importance.

The structure of electrical trees can be extremely fine and is, therefore, often difficult to image optically in semi-crystalline polymers, as a consequence of light scattering processes. Light scattering within a non-absorbing medium is primarily associated with the changes in local refractive index that are associated with phase boundaries or particular structural features, when these have dimensions that are comparable to the wavelength of light [8]. In semi-crystalline polymers, spherulitic development is therefore particularly important and, for this reason, increases in optical clarity are often associated with enhanced nucleation and a corresponding reduction in spherulite size. Although

* Corresponding author. Department of Electronics and Computer Science, University of Southampton, Highfield, Southampton SO17 1BJ, UK.

0032-3861/01/$ - see front matter
PII: S0032-3861(01)00031-3

the onset of crystallization has been studied in many polymeric systems [9–11], the incorporation of nucleating additives has most notably been considered in connection with polypropylene or related copolymers. In these materials, spherulitic development can be extensive and its control is therefore a significant technological issue [11–13]. Nevertheless, little detailed morphological work has been performed to investigate how clarifying additives interact with and modify the structure of the host polymer. The relationships between crystallization conditions, morphology and properties in these systems are therefore unclear.

This paper describes a detailed study of the morphology and thermal behaviour of a commercial, clarified propylene/ethylene copolymer. Since our ultimate interest in this material stems from its potential as a model system for studies of dielectric breakdown through the growth of electrical trees, as a precursor to this, the effect of the observed morphological variations on the electric strength of the material is described. In addition, since Stark and Garton [14] first proposed an electromechanical mechanism for dielectric breakdown in 1955, such ideas have attracted considerable attention [15]. Thus, relationships between mechanical properties and electrical failure are also explored.

2. Experimental

2.1. Materials and sample preparation

The results reported here focus on the sorbitol-clarified propylene/ethylene copolymer, Novolen 3200MC (BASF plc). Such materials typically contain ethylene comonomer of the order of 3% and about 2000 ppm of the clarifying additive. The infra-red absorption, crystallization and melting behaviour of the equivalent unclarified grade, Novolen 3240NC, [16] are all consistent with this ethylene content [17,18]. Gel permeation chromatography (GPC) after solvent extraction of the clarifying agent gave average molecular mass values of $M_w = 1.9 \times 10^5$ and $M_n = 5.2 \times 10^4$.

Samples for microscopy and thermal analysis were prepared by melting the pelletized polymer between a slide and a cover slip on a Koffler hot bench at 200°C; they were then moved to a Mettler FP52 hotstage and crystallized at the desired temperature (T_c). The process of crystallization was observed optically and, when complete, the samples were finally quenched into ice/water. Specimens for electrical testing were prepared using a Graseby Specac model 25.011 press equipped with a thin film maker. Material was pressed into thin discs with a thickness of 75 μm and, then, either quenched directly in ice/water or crystallized isothermally in a silicone oil bath at the desired temperature. Samples for mechanical testing were moulded into plaques, using a flat-plate press, and then isothermally crystallized under the same conditions as described above for the preparation of the thin disc specimens.

2.2. Characterisation methods

Samples for electron microscopy were treated with a permanganic etching reagent developed at Reading [19,20]. Microtomed surfaces were typically etched for 2 h with a 1% w/v solution of potassium permanganate in an acid mix composed of 10 parts concentrated sulphuric acid to 4 parts dry phosphoric acid to 2 parts water, and then recovered using standard procedures. From the etched surfaces, two-stage indirect replicas were prepared. These samples were observed using a Phillips EM301 transmission electron microscope (TEM) operating at 80 kV.

The material's melting behaviour was studied as a function of thermal history using a Perkin–Elmer DSC-2C differential scanning calorimeter (DSC). The instrument was routinely calibrated with high purity indium and all data acquisition and analysis were performed using an MC^2 Thermal Systems software package.

Electrical breakdown testing was performed according to our standard ramp testing procedure [7], which is in line with the ASTM standard D149-87. The sample was immersed in Dow Corning 200/20cs silicone oil, between opposing 6.3 mm diameter steel ball bearings. The lower electrode was connected to earth and an increasing AC voltage was applied to the upper electrode at a ramp rate of 50 V/s, until the sample failed. All experimental parameters were computer controlled and appropriate data were logged automatically. Twenty breakdown tests were performed on each system, from which, the mean strength plus 95% confidence intervals were calculated.

Mechanical testing was carried out with a Monsanto T2000 tensile tester, using dumb-bell specimens cut from moulded sheets. The dimensions of the test specimens in the gauge region were: length 20 mm, width 1.5 mm and thickness 1.5 mm. All samples were drawn at room temperature, using a cross-head speed of either 25 or 100 mm/min. For each set of crystallization conditions, at least 5 samples were tested.

3. Results and discussion

3.1. Melting behaviour

Fig. 1 shows the DSC melting behaviour of the clarified propylene/ethylene copolymer as a function of crystallization temperature, as recorded at 10 K/min. Multiple peaks are apparent in all the traces. For the quenched sample, two overlapping peaks are observed (marked I and R), whereas the isothermally crystallized specimens generally exhibit a number of separate endotherms. These are labelled Q, S and P in the trace from the 134°C crystallized specimen; for $T_c < 128$°C the peak marked Q is absent. In the isothermal specimens, the S-peak is situated just above the crystallization temperature and, as a consequence, is generally at a lower temperature than either of the two overlapping

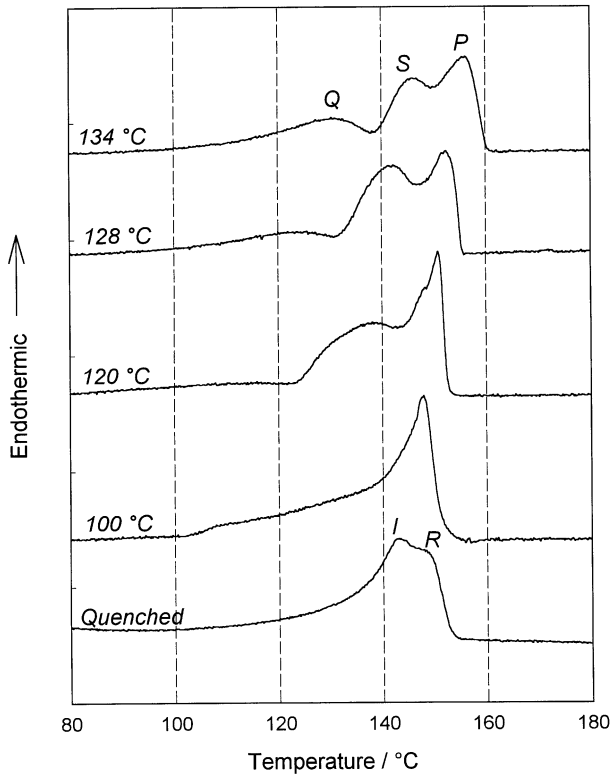

Fig. 1. DSC melting behaviour of the clarified propylene/ethylene copolymer as a function of crystallization temperature. The DSC scan rate is 10 K/min.

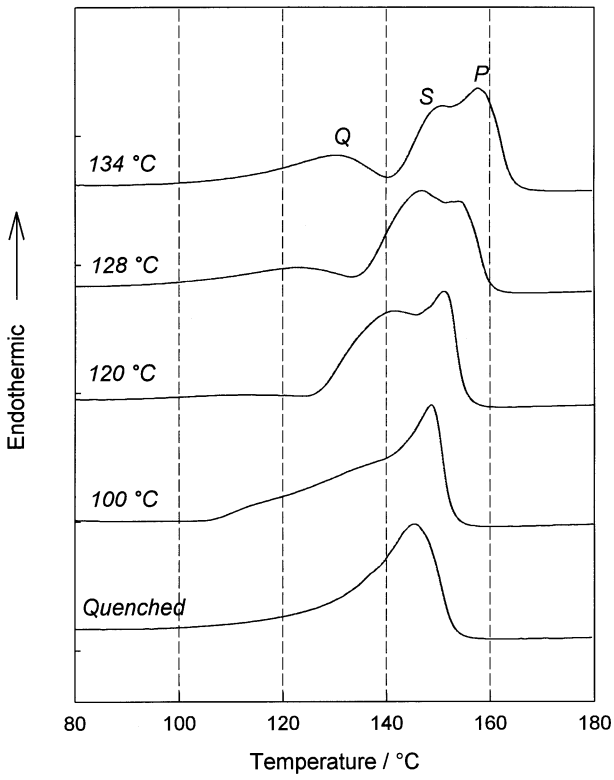

Fig. 2. DSC melting behaviour of the clarified propylene/ethylene copolymer as a function of crystallization temperature. The DSC scan rate is 40 K/min which, in comparison with Fig. 1, accounts for the apparent displacement of all traces to higher temperatures.

peaks which characterize the quenched sample. A number of factors must therefore contribute to the melting behaviour of this material. From DSC results obtained at 40 K/min (Fig. 2), it can be seen that only a single peak, equivalent to I in Fig. 1, appears in the trace from the quenched sample. Multiple peaks still exist for all the isothermal specimens. These results indicate that the high temperature shoulder in the quenched sample in Fig. 1 (peak R) arises from reorganisation during heating, since the sample was unable to crystallize perfectly when quenched into ice/water. Conversely, for the isothermal specimens, the highest temperature peak (equivalent to peak P) cannot be a consequence of recrystallization, since the magnitude of this feature is not systematically diminished by the increase in scan rate. We therefore propose that the highest temperature peak in each isothermal trace results from the fusion of crystallites that developed during primarily crystallization. The remaining isothermally grown material is then most reasonably associated with some secondary crystallization process. This analysis is further supported by the evolution of melting behaviour as a function of crystallization time at 134°C, as shown in Fig. 3. This indicates that both lamellar populations develop isothermally, since none of these specimens were quenched prior to melting. After 7 min, there is already evidence of the upper peak, whereas secondary crystallization is only apparent after 15 min. This primary crystallization is most probably associated with the longer propylene sequences present within the copolymer. At this point we do not seek to define precisely the terms primary and secondary crystallization as they relate to this system. We will therefore return to this point in due course.

The above analysis is consistent with ideas of molecular fractionation previously applied to relatively defective polypropylenes [21–23], and is in agreement with the more recent report by Feng and Hay of the melting behaviour of fractions extracted from a random propylene/ethylene copolymer [24]. However, it contradicts many other studies of the melting behaviour of the isotactic homopolymer, where most authors have attributed similar multiple peaks to dynamic reorganization effects in the DSC [22]. Laihonen et al. [17,18] examined the crystallization, melting and structure of a series of propylene/ethylene copolymers with varying ethylene contents. They observed the presence of both α and γ crystal forms [25] and showed how the relatively low melting temperature of the γ crystals [18] could be another factor leading to multiple melting peaks. However, from this work, it was concluded that the γ crystal form tends to develop at relatively low temperatures from systems with a higher ethylene content than is present in Novolen 3200MC (i.e. greater than 3%). Consequently, it would appear that such structures are unlikely to contribute

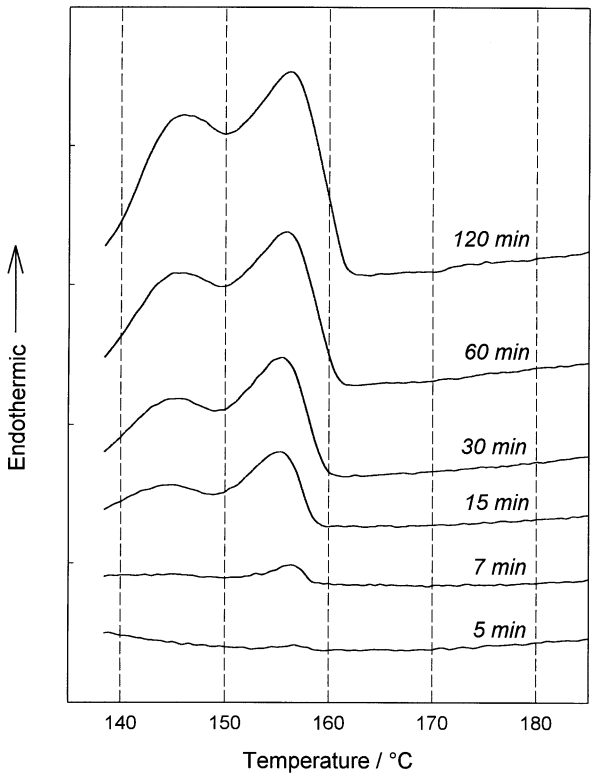

Fig. 3. DSC melting behaviour of samples crystallized at 134°C for various times; all samples were heated directly from the isothermal crystallization temperature. DSC scan rate is 10 K/min.

to the multiple melting peaks which, in Fig. 1, are best resolved when $T_c > 128$°C. Conversely, appreciable γ contents have recently been observed in a copolymer containing ~3% ethylene, particularly when crystallized in the presence of a sorbitol-based clarifier [26], as employed here. However, since we are not able to detect γ crystals in our systems by wide angle X-ray scattering, we do not believe that their presence is central to the DSC behaviour reported here.

It should also be noted that a third peak appears below T_c (equivalent to peak Q in Fig. 1), when the crystallization temperature is 128°C or above. Although it has been demonstrated that some ethylene units can become incorporated within the crystal lattice [17], since this peak corresponds to a molecular fraction that is unable to crystallize at such high temperatures, it is probably associated with the most ethylene-rich molecular segments. This behaviour suggests that appreciable molecular segregation occurs at 128°C and above, as observed by Laihonen et al. [18].

3.2. Morphology

Fig. 4 shows samples of the equivalent unclarified propylene/ethylene copolymer, Novolen 3240NC, crystallized isothermally at 100°C and 128°C. As discussed elsewhere [16], the precise morphology that develops in this system can be dependent upon the material's exact thermal history;

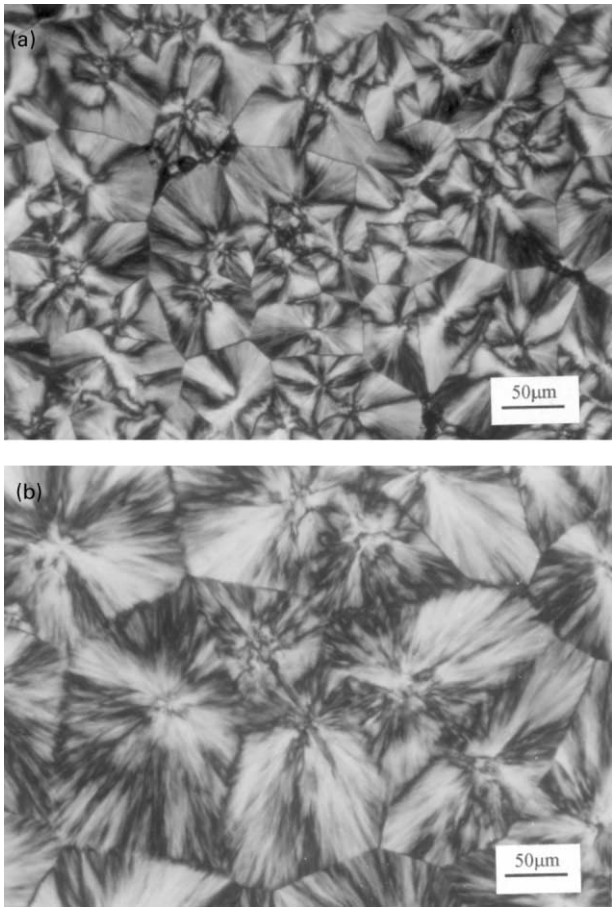

Fig. 4. Transmission optical micrographs (crossed polars) showing the typical spherulitic morphology that develops in the equivalent propylene/ethylene copolymer in the absence of the clarifier. Both samples were melted at 200°C before being crystallized isothermally at (a) 110°C and (b) 128°C.

these samples were initially melted at the same temperature used to prepare the clarified samples. The extensive spherulitic structures shown in Fig. 4, which are entirely in line with those which develop in propylene-based polymers [27–29], can therefore can considered as being typical of those which develop in this material. Fig. 4 therefore, provides a reference point from which to judge the morphological effect of the clarifier.

Representative electron micrographs of clarified samples are shown in Fig. 5. The lamellar morphology of the quenched material is rather indistinct, as can be seen in Fig. 5a; few extensive crystallites appear to form under such conditions. Crystallization at 100°C (Fig. 5b) gives a clear lamellar structure although, again, no larger scale structural units can be observed. However, a so-called cross-hatched arrangement of lamellae [25] can also be seen in places, indicating the presence of the α crystal form of polypropylene. The morphology described above is in sharp contrast to the equivalent specimen shown in Fig. 4a, a change that is a direct consequence of the action of the clarifier. Sorbitols constitute a family of

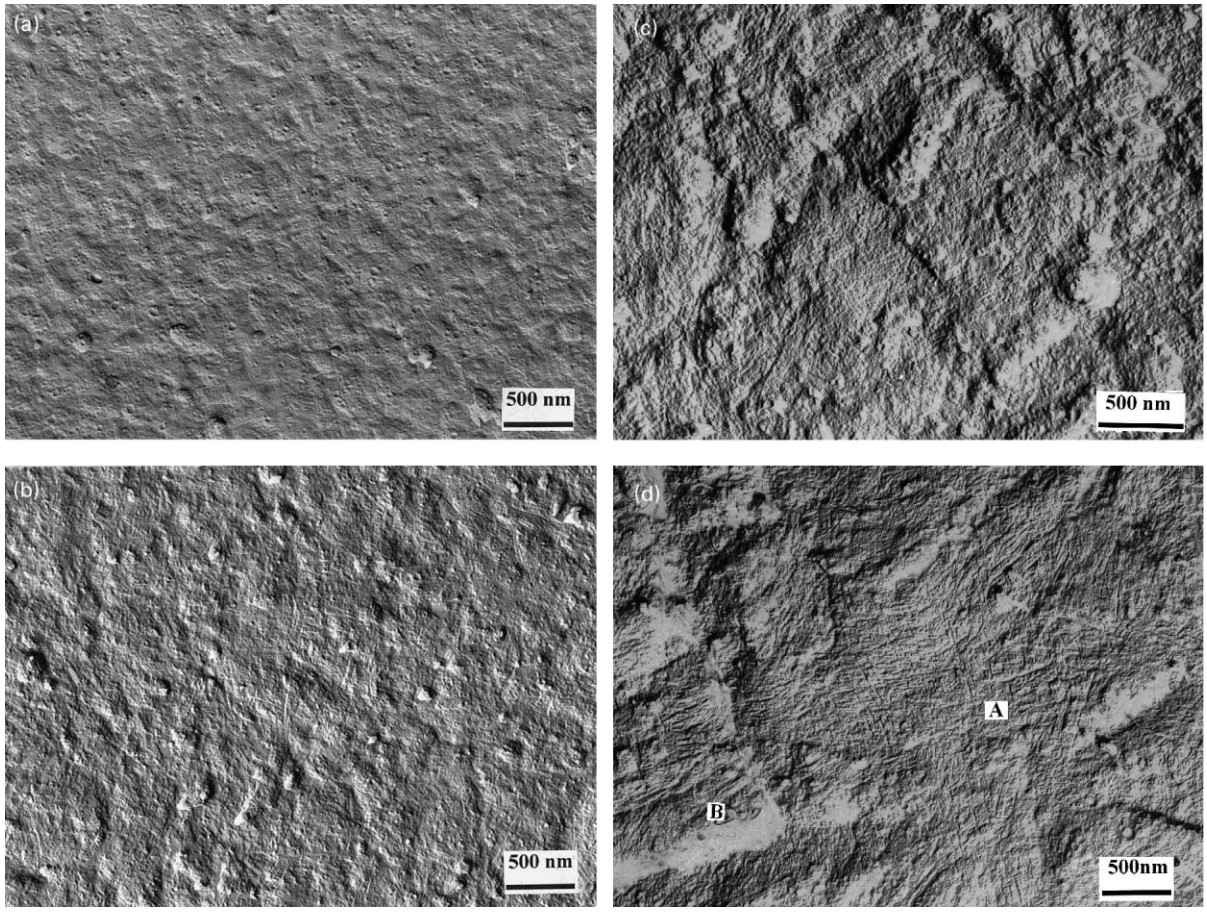

Fig. 5. Transmission electron micrographs showing the effect of crystallization temperature on morphology. Samples were crystallized (a) by quenching into ice/water or by isothermal crystallization to completion at (b) 100°C, (c) 128°C and (d) 134°C.

organic compounds which dissolve readily in many molten polyolefins. At appropriate temperatures (~150°C), they crystallize within the polymer melt to form a disperse gel with an extremely high surface area to volume ratio. As a result of some epitaxial interaction between the sorbitol gel and the crystallizing molecules, which is not well understood, the gel can induce massive nucleation of the polymer [30–32], such that large-scale structures such as spherulites do not have sufficient volume to develop. The sample crystallized at 120°C exhibits an identical morphology to that shown in Fig. 5b and is, therefore, omitted for the sake of brevity.

As the crystallization temperature is increased further (as shown in Fig. 5c and d), the lamellae become thicker and, more importantly, the morphology becomes much coarser. At A in Fig. 5d, for example, extensive lamellar crystals can be seen edge-on, which are separated from one another by cross-hatching. This abrupt change in overall morphology indicates that the nucleating efficiency of the clarifier is highly temperature dependent, a result which questions the relevance of common practice in which dynamic crystallization techniques are used to assess the relative nucleating efficiencies of different additive systems [32]. However, the most striking morphological consequence of crystallization at such high temperatures is the presence of the rather featureless elongated regions (for example at B), which do not appear to relate to the surrounding lamellar texture in any simple way. These features, which are several microns in length, are particularly apparent in Fig. 6, which shows a 134°C crystallized sample at a lower magnification.

From the above DSC results, it is clear that, at high temperatures, the ethylene-rich components of the melt cannot solidify and are excluded from the less defective crystallizing phase. Clearly, the extent to which molecular fractionation can occur will be influenced by kinetic factors and, in this case, both the higher crystallization temperature and the reduced nucleation density will contribute to a reduction in the overall crystallization rate. In turn, this provides more scope for molecular segregation and the consequent evolution of hierarchical morphologies. Nevertheless, the nature and association of the structural units that constitute the morphology shown in Fig. 5 are not clear, particularly when the topography of this etched surface is considered in some detail. In addition, how do these various features relate to the multiple-peak DSC endotherms described above?

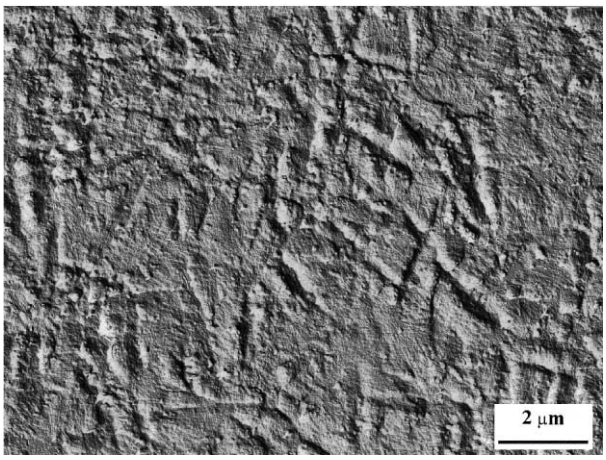

Fig. 6. Low magnification transmission electron micrograph showing the rough surface topography that typifies high temperature crystallization in this clarified propylene/ethylene copolymer. The sample was crystallized to completion at 134°C.

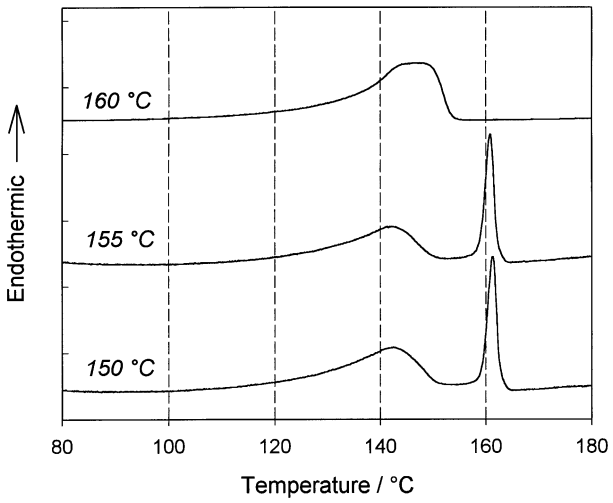

Fig. 7. DSC melting behaviour of samples first crystallized to completion at 134°C and then annealed for 20 min at the indicated temperatures. DSC scan rate is 10 K/min.

Crystallization of propylene-based polymers generally results in the formation of spherulites of the type shown in Fig. 4 or, when growth is particularly slow, so-called quadrites [33]. It would therefore seem reasonable to suppose that defective molecular fractions would be rejected during the development of such structures and could therefore lead to the formation of a low crystallinity phase at interspherulitic boundaries. Indeed, the crystallization of blends of linear and branched polyethylenes under analogous conditions (where only the linear component undergoes slow crystallization), often leads to the formation of distinct inter-spherulitic regions, even when isothermal crystallization is allowed to continue to completion [7]. When such morphologies are treated with permanganic reagents, differential etching rates can be high and rough surfaces can result. However, in Fig. 6, such an explanation cannot be correct since, by considering the shadow contrast in detail, it is apparent that the extended structures, which are the dominant features in such micrographs, are etched less than the intervening material. To explore more fully the origins of these structural units, samples previously crystallized at 134°C were partially melted, such that the spatial location of the primary, secondary and quenched lamellae could be explored.

Fig. 7 shows three DSC melting traces obtained from specimens that had been crystallized fully at 134°C, as above. Subsequent to this, each was then annealed for 20 min at 150, 155 or 160°C before, finally, being quenched. Such a procedure, in which the material is heated to a temperature near the local endothermic heat flow minimum between peaks S and P in Fig. 1, would, ideally, melt the secondary crystals but leave varying proportions of the primary population unchanged. Clearly, the former objective has been met. No evidence of secondary crystals remains and the endotherm at ~140°C in each trace in Fig. 7 is comparable with the melting behaviour of the quenched specimens in Figs. 1 and 2. However, it is equally evident that, when annealed at 150 or 155°C, the primary lamellae thicken appreciably, since their final melting peaks are sharper and exhibit higher peak maxima than peak P in Fig. 1. This observation demonstrates that reorganization effects can occur in this material and, at first sight, may appear to question our previous assertion that the multiple melting peaks seen by DSC do genuinely reflect the initial lamellar populations present in each material. However, Fig. 7 also demonstrates that, when a sample is heated directly to 160°C, its subsequent endotherm is equivalent to that of the quenched specimen in Fig. 1. That is, it melts completely. Taken together, these results indicate that the formation of lamellae which are thermally stable at temperatures in excess of 160°C requires prolonged annealing at a high temperature (e.g. 150–155°C). This does not occur in the DSC, particularly at a scan rate of 40 K/min.

The effect on the morphology of partial melting followed by quenching is shown in Fig. 8. In both of these micrographs, extensive lath-like lamellar crystals can be seen extending for several microns. Since, from Fig. 5a, such extensive structures do not form on quenching, these crystals must represent the remnant fraction of the initial structure; that is, the primary lamellae. Arrowed in Fig. 8a, for example, these can be seen in an edge-on orientation whereas, in Fig. 8b, similar crystals can be seen flat on. Also, in both figures, there is evidence of these lamellae being organized into quadrites. At X in each micrograph are two of the radiating skeletal arms of such a structure. These features are defined by considerable relief within the etched surface and, within each object, are separated by regions in which the lamellar texture is less well defined. The cross-hatching, which, in the initial morphology is

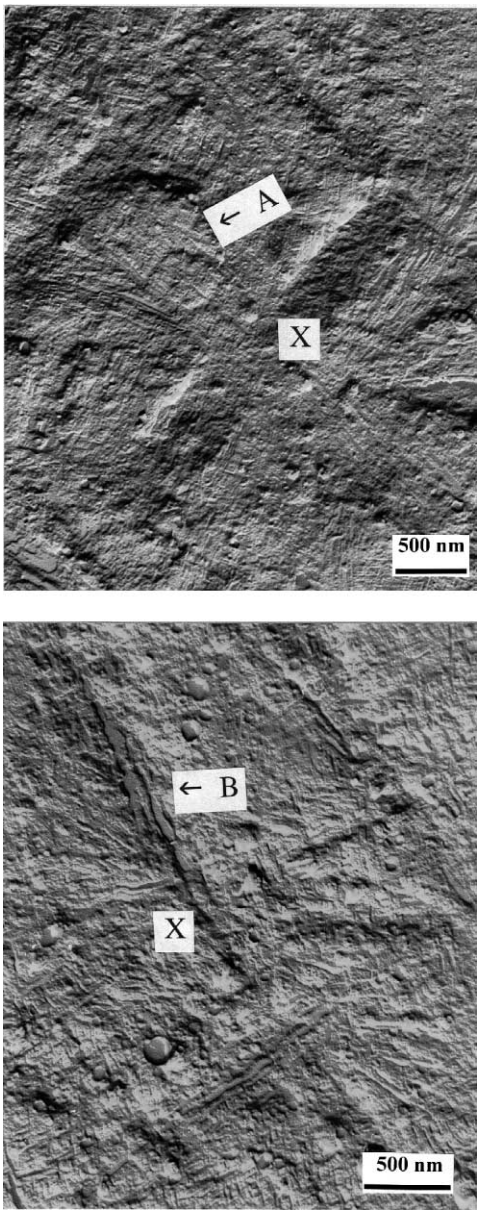

Fig. 8. Transmission electron micrographs showing the effect of annealing temperature on the morphology of a sample first crystallized to completion at 134°C: annealing temperatures are (a) 150°C and (b) 155°C.

clearly defined, is significantly reduced after partial melting. These observations, when combined with previous morphological and DCS data, enable the growth process at 134°C to be described fully. To summarize:

(i) Partial melting experiments demonstrate that the highest melting lamellar population, equivalent to peak P in the DSC endotherm, corresponds to extensive, lath-like lamellae which constitute the primary, radiating lamellar skeleton of quadrites.

(ii) These primary lamellae grow outward and initiate the formation of cross-hatching, which develops to fill the space between the skeletal arms of the structure. From the clarity of the cross-hatched texture in Fig. 5d, in comparison with structures which developed on quenching (Fig. 5a), it is clear that this morphological element forms isothermally. However, the fact that it is largely destroyed at 155°C, somewhat less so at 150°C, leads to the conclusion that these lamellae correspond to the secondary crystallization seen by DSC (peak S in Fig. 1). The reduced thermal stability of these later forming crystals is consistent with them having developed in a more constrained environment [34] or from less crystallizable material than the primary population [7,35].

(iii) The extended linear structures seen in Figs. 5 and 6 are therefore explained in terms of impinging quadrites viewed in a variety of orientations. That such local variations can give rise to such pronounced surface topographical features, is demonstrated clearly in the following paper [16]. Similarly, comparison of Figs. 5d and 8a reveals why these structures could not be easily recognized in the original material, prior to partial melting. Whilst the morphological signature of quadrites is readily identified when they are isolated and viewed edge-on (pseudo-rectangular shape and internal cross-hatched texture [35,36]), when crystallization proceeds to completion, impingement of neighbouring objects may serve to modify their characteristic out-line. Additionally, profuse overgrowth upon the primary laths via cross-hatching can mask the underlying crystal habit.

(iv) The most defective (i.e. ethylene-rich) molecular segments are unable to crystallize at such high temperatures. However, we have not observed any macroscopic phase separation consistent with the magnitude of the quench peak seen in the 134°C crystallized sample in Fig. 1. Consequently, we suggest that the bulk of this component, being unable to crystallize at these high temperatures, becomes segregated between individual isothermal lamellae and then crystallizes on quenching. Some material may, additionally, be rejected to accumulate at the boundaries between neighbouring quadrites but, since we have observed no clear evidence of such macroscopic phase separation, this can only be a relatively minor component. Nevertheless, the mere existence of boundaries between distinct morphological elements is significant, differentiating morphologies which form at 128°C and above from the continuous lamellar textures that develop at lower temperatures.

The above results demonstrate the role of molecular fractionation, combined with variations in nucleation density, in determining the morphology of this clarified propylene/ethylene copolymer. The extent to which lamellar aggregates are able to form is temperature dependent and whilst we have, thus far, concentrated on exploring the nature of these microstructures, the impinged quadrite morphologies which characterize the high temperature crystallization of this material should have important consequences for the macroscopic physical properties of the material.

3.3. Dielectric breakdown

Fig. 9 shows the average electric breakdown strength of

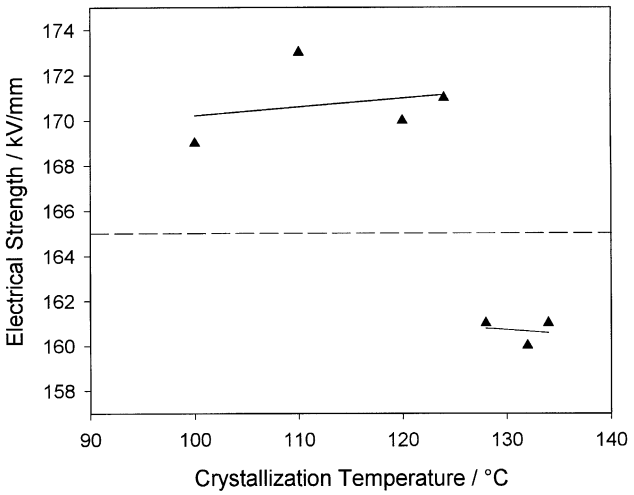

Fig. 9. Electric strength of the clarified propylene/ethylene copolymer as a function of isothermal crystallization temperature. The dashed line represents the average breakdown strength obtained from samples quenched into ice/water and, for each point, the calculated 95% confidence interval is $\sim \pm 4$ kV/mm.

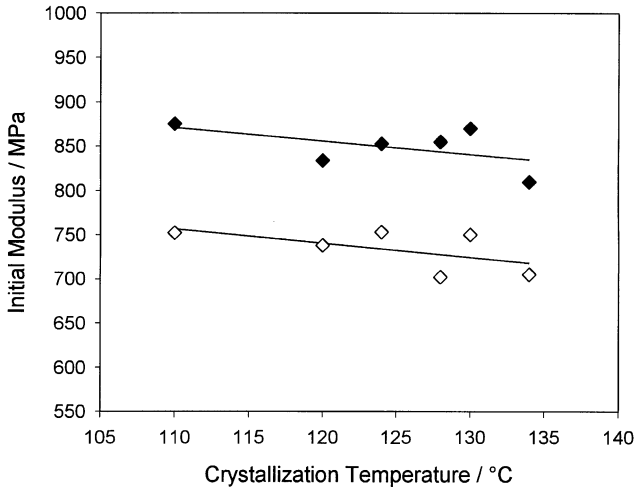

Fig. 10. Initial modulus (measured up to 2% strain) as a function of crystallization temperature, at strain rates of (◇) 25 and (◆) 100 mm/min.

this system as a function of crystallization temperature. Up to 124°C, the value of the electric strength obtained from the isothermally crystallized materials effectively remains constant at ~170 kV/mm (the 95% confidence interval for all of these data is typically ±4 kV/mm). This value is slightly above that of the quenched system, whose strength, to aid comparison, is indicated by the dashed horizontal line in Fig. 9. However, the electric strength decreases significantly when the sample is crystallized at 128°C and, thereafter, remains constant at ~160 kV/mm.

The above morphological results demonstrate that isothermal crystallization below 128°C leads to the formation of fine, uniform lamellar morphologies. Although the morphology of the quenched sample is also uniform, the crystallinity is reduced, thereby providing a probable explanation of the relatively low electric strength of that material [37]. When crystallized above 128°C, the morphology becomes coarser and boundary regions were shown to form. From Fig. 9 it is clear that this morphological transition is accompanied by a reduction in electric strength. Considering these results in concert, it is evident that, whilst electric strength can be improved by increasing crystallinity (i.e. through controlled isothermal crystallization as opposed to quenching), the spatial location of crystallites is more important. As in our previous studies of polyethylene blends [7], this demonstrates that morphological factors do markedly influence the electric strength of semi-crystalline polymers.

3.4. Mechanical properties

Fig. 10 shows initial Young's modulus, plotted as a function of crystallization temperature. Comparing the open and solid diamonds (data collected at strain rates of 25 and 100 mm/min, respectively), it is evident that, for any given material, the absolute value of this parameter is strongly dependent on the chosen experimental conditions. The measured modulus is appreciably higher at the higher strain rate. However, the modulus does not appear to change markedly with crystallization temperature and, in particular, does not show any abrupt change when T_c is of the order of 128°C. Equivalent plots showing yield and ultimate failure stress values are shown in Fig. 11. At the lower rate (25 mm/min — open symbols), the two parameters lie close to one another and both decrease somewhat as the crystallization temperature is increased. These data have therefore been considered as a single set, which is represented by the best-fit straight line that is shown. However, at the higher strain rate (100 mm/min — solid symbols), the measured failure stress is much lower than the yield stress. Whilst none of the above data show evidence of morphological effects, the decrease in failure stress between 120 and 130°C could, possibly, be related to the morphological transition that occurs at ~128°C. Nevertheless, by inspection of the other data sets it is clear that these mechanical parameters contain appreciable uncertainties. For consistency with the electrical data presented above, 95% confidence intervals for these parameters range from 3–15%. Consequently, a straight line fit to all the above data sets is the only statistically valid approach when this evidence is viewed in isolation.

The variation of ultimate failure strain with crystallization temperature is shown in Fig. 12. In this, more convincing evidence is apparent for a morphological effect. At the lower strain rate, the failure strain decreases monotonically with increasing T_c, as in the case of the parameters described above. However, the higher speed data show clear evidence of a change in properties at 128°C. Thus, it would appear that, in the system considered here, the pronounced morphological

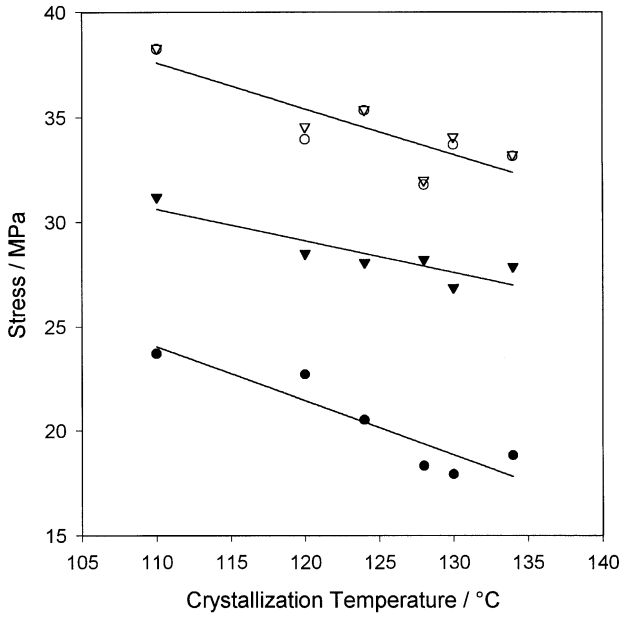

Fig. 11. Effect of crystallization temperature on yield stress (▽ 25 mm/min strain rate and ▼ 100 mm/min) and ultimate stress at failure (○ 25 mm/min strain rate and ● 100 mm/min).

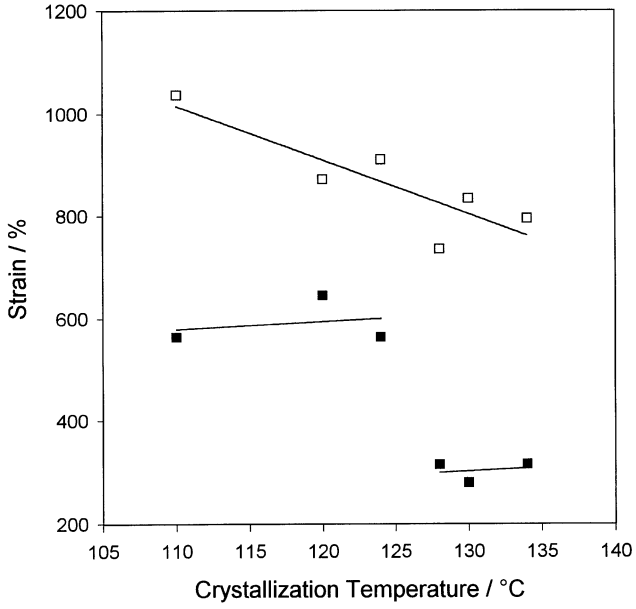

Fig. 12. Effect of crystallization temperature on ultimate failure strain as measured at strain rates of (□) 25 and (■) 100 mm/min.

change resulting from the reduced efficiency of the clarifier at high crystallization temperatures only manifests itself in the ultimate failure of the material (i.e. failure strain and, less obviously, failure stress) and, then, only when deformation occurs rapidly.

From the above results it is evident that macroscopic mechanical properties are dependent on experimental conditions but, unlike electric strength, neither the modulus, yield stress nor yield strain appear to reflect the morphological variations that exist in this system. In view of the extent of the structural changes described above, this result is surprising. The consequent fact that certain key mechanical parameters do not parallel our electric strength data also appears inconsistent with previous studies described in the literature [14,15,38,39], where positive correlations between dielectric breakdown behaviour and mechanical properties have been reported.

Based upon concepts of fracture mechanics [40], two electro-mechanical mechanisms have been proposed to explain certain aspects of the dielectric breakdown behaviour of insulators. One, the electro-fracture mechanism of Zeller et al. [41,42], appears feasible as an electrical ageing mechanism and involves the growth of a filamentary crack through a dielectric. This occurs as a result of the release of electrostatic energy under conditions where it exceeds the electromechanical energy. This model ultimately involves the yield stress, rather than any other mechanical factors, and predicts that the electric strength will vary as the stress to the power of one half. Another is the filamentary electro-mechanical breakdown model of Fothergill [43], which considers rapid breakdown rather than ageing. This predicts that the electric strength of a material will be proportional to its Young's modulus to the power of one quarter.

To investigate the relevance of such models to our data, various log–log plots of electric strength against mechanical parameters were generated. The only significant correlations that were found involved ultimate failure properties, as measured at a strain rate of 100 mm/min. Fig. 13 includes both the high strain-rate failure stress and strain plotted against electric strength, which demonstrates that it is possible to correlate certain mechanical and electrical properties. However, the quantities involved and the exponents that can be derived from the gradients do not concur with existing theories.[1] Nevertheless, Fig. 13 does lend some weight to the general concept that dielectric breakdown involves a mechanical element, rather than being a uniquely electrical phenomenon. Further work is, however, required.

4. Conclusions

The crystallization behaviour and morphology of a propylene/ethylene copolymer has been shown to be affected significantly by the addition of a clarifying agent, such that normal spherulitic development is completely suppressed. When crystallization occurs below 128°C, a uniform lamellar morphology results from the profuse nucleation that is induced by the clarifier. These lamellae are thermally stable and, as a consequence, do not reorganized extensively during heating in the DSC. Two distinct lamellar populations are evident, both of which develop

[1] These plots suggest that the failure stress varies as $(E_b)^{0.32}$, where E_b is the electric strength. The failure strain varies as $(E_b)^{0.10}$.

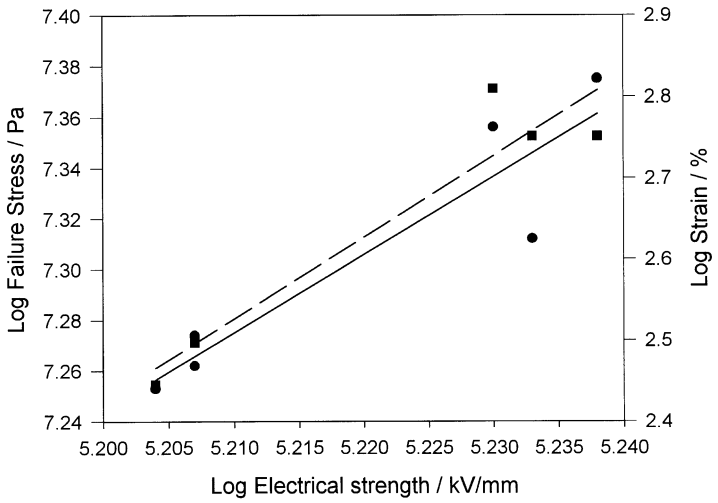

Fig. 13. Plot of ultimate failure stress (● solid line) and ultimate failure strain (■ dashed line) against electric strength. All the mechanical data shown were recorded at 100 mm/min.

isothermally. At 128°C and above, nucleation is more sporadic and this, combined with the requirement for more perfect molecular sequences, results in the sequential growth of a lamellar hierarchy. In this temperature range, DSC evidence indicates the presence of primary, secondary and quenched lamellae. The primary crystallization involves the growth of extensive lath-like lamellae, which form the radiating skeletal arms of quadrites. These are separated by typical cross-hatched overgrowths, which are associated with secondary, isothermal crystallization. Finally, a distinct ethylene-rich phase develops, which crystallizes on quenching, between individual isothermal lamellae.

The marked change in morphology described above is accompanied by an associated change in the electric strength of the material. In comparison with rapid quenching, isothermal crystallization results in increased crystallinity and, provided both processes give equivalent morphologies (continuous and uniform lamellar textures), this confers an increase in electric strength on the system. However, the development of quadrites, in conjunction with molecular segregation processes, necessarily means that distinct boundaries result where one quadrite impinges upon its neighbours. This morphology in general, and the boundaries in particular, then results in a significant decrease in electric strength. As in our previous studies of polyethylene blends, it is the spatial location of lamellae rather than simple globally averaged parameters such as crystallinity that determines the short-term breakdown behaviour of a specimen. However, longer-term failure processes involve the initiation and propagation of electrical trees. In view of the morphological variations described above, Novolen 3200MC constitutes an ideal model system in which to perform dynamic studies of tree growth. Not only can it exhibit excellent optical clarity, when crystallized below 128°C, but the marked change in structure that occurs at about this temperature enables the effect of morphology on tree growth to be explored in structurally different but chemically identical systems. This work is described elsewhere [44].

Our mechanical measurements indicate that experimental conditions markedly influence the data that is obtained. In most cases, parameters vary continuously with crystallization temperature, despite the discontinuous nature of the morphological changes described above. Consequently, these mechanical results could not, in general, be related to our electric strength measurements. Nevertheless, both the ultimate failure stress and strain did appear to mirror the variations seen in electric strength. However, even here, the relationships did not conform to theoretical predictions. Consequently, we can only suggest that, whilst dielectric breakdown may well involves a mechanical element, the process is not as simple as existing theories would imply.

Acknowledgements

The support of National Grid and its permission to publish this paper are gratefully acknowledged.

References

[1] Wagner H. Ann Rep Conf Electr Insul Diel Phenom 1974:62.
[2] Phillips PJ. IEEE Trans Elec Insul 1978;EI-13:451.
[3] Barnes SR. Polymer 1980;21:723.
[4] Kolesov SN. IEEE Trans Elec Insul 1980;EI-15:382.
[5] Fukuda T, Irie S, Asada Y, Maeda M, Nakagawa H, Yamada N. IEEE Trans Elec Insul 1982;EI-17:386.
[6] Ceres BV, Schultz JM. J Appl Polym Sci 1984;29:4183.
[7] Hosier IL, Vaughan AS, Swingler SG. J Mater Sci 1997;32:4523.
[8] Bodor G. Structural investigation of polymers. Chichester, UK: Ellis Horwood, 1991.

[9] Reinsch VE, Rebenfeld L. J Appl Polym Sci 1994;52:649.
[10] Lednicky F, Muchova M. J Macromol Sci; Phys 1995;B34:75.
[11] Thierry A, Fillon C, Straupé C, Lotz B, Wittmann JC. Progr Colloid Polym Sci 1992;87:28.
[12] Sterzynski T, Lambla M, Crozier H, Thomas M. Adv Polym Technol 1994;13:25.
[13] Gahleitner M, Wolfschwenger J, Bachner C, Bernreitner K, Neissl W. J Appl Polym Sci 1996;61:649.
[14] Stark KH, Garton CG. Nature 1955;24:1225.
[15] Dissado LA, Fothergill JC. Electrical degradation and breakdown in polymers. London: Peter Peregrinus, 1992. p. 263.
[16] Zhao Y, Vaughan AS, Sutton SJ, Swingler SG. Polymer 2001;42:6605.
[17] Laihonen S, Gedde UW, Werner PE, Martinez-Salazar J. Polymer 1997;38:361.
[18] Laihonen S, Gedde UW, Werner PE, Westdahl M, Jääskeläinen P, Martinez-Salazar J. Polymer 1997;38:371.
[19] Olley RH, Hodge AM, Bassett DC. J Polym Sci; Phys 1979;17:627.
[20] Olley RH, Bassett DC. Polymer 1982;23:1707.
[21] Martuscelli E, Pracella M, Crispino L. Polymer 1983;24:693.
[22] Paukkeri R, Lehtinen A. Polymer 1993;34:4083.
[23] Yadav YS, Jain PC. Polymer 1986;27:721.
[24] Feng Y, Hay JN. Polymer 1998;39:6589.
[25] Khoury F. J Res Nat Bur Stand 1966;70A:29.
[26] Goldbeck-Wood G. Private communication.
[27] Padden FJ, Keith HD. J Appl Phys 1959;30:1479.
[28] Norton DR, Keller A. Polymer 1985;26:704.
[29] Schönherr H, Snétivy D, Vansco J. Polym Bull 1993;30:567.
[30] Shepard TA, Delsorbo CR, Louth RM, Walborn JL, Norman DA, Harvey NG, Spontak RJ. J Polym Sci; Phys Ed 1997;35:2617.
[31] Thierry A, Straupé C, Lotz B, Wittmann JC. Polym Commun 1990;31:299.
[32] Fillon B, Thierry A, Lotz B, Wittmann JC. J Therm Anal 1994;42:721.
[33] Binsbergen FL, De Lange BGM. Polymer 1968;9:23.
[34] Bassett DC, Olley RH, Al Raheil IAM. Polymer 1988;29:1745.
[35] Bassett DC. CRC Crit Rev Solid State Mater Sci 1984;12:97.
[36] Olley RH, Bassett DC. Polymer 1989;30:399.
[37] Ieda M. IEEE Trans Elec Insul 1980;EI-15:206.
[38] Hikita M, Tajima S, Kanno I, Ishino I, Sawa G, Ieda M. Jpn J Appl Phys 1985;24:988.
[39] Auckland DW, Varlow BR. IEE Proc A — Sci Measmt Technol 1991;138:51.
[40] Griffith AA. Phil Trans R Soc Lond A 1920;221:163.
[41] Zeller HR, Hibma T, Pfluger P. Ann Rep Conf Electr Insul Diel Phenom 1984:85.
[42] Zeller HR, Schneider WR. J Appl Phys 1984;56:455.
[43] Fothergill JC. IEEE Trans Elec Insul 1991;EI-26:1124.
[44] Champion JV, Dodd SJ, Zhao Y, Vaughan AS, Brown M, Davies AE, Sutton SJ, Swingler SG. IEEE Trans Diel Electr Insul 2001;DEI-8:284.